Novel Therapeutic Anti-ADAM17 Antibody A9(B8) Enhances EGFR-TKI–Mediated Anticancer Activity in NSCLC

Zheng Yang[*], Kin Iong Chan[†,‡], Hang Fai Kwok[*,†] and Kin Yip Tam[*]

[*]Cancer Centre, Faculty of Health Sciences, University of Macau, Avenida de Universidade, Taipa, Macau SAR, PR China; [†]Centre for Precision Medicine Research and Training, Faculty of Health Sciences, University of Macau, Avenida de Universidade, Taipa, Macau SAR, PR China; [‡]Department of Pathology, Kiang Wu Hospital, Macau SAR, PR China

Abstract

Epidermal growth factor receptor (EGFR) mutations were found in 30%-40% of non–small cell lung cancer (NSCLC) patients, who often responded well to EGFR tyrosine kinase inhibitors (EGFR-TKIs) as exemplified by erlotinib and gefitinib in the past decades. However, EGFR mutation-led drug resistance usually occurred upon prolonged treatment with EGFR-TKI. Herein, we study the anticancer effects of EGFR-TKI in combination with a newly developed antibody, A9(B8), to target a disintegrin and metalloprotease (ADAM) 17 that was overexpressed in NSCLC patients. NSCLC cell lines with different EGFR mutations were used to evaluate the drug combination. We have found that the EGFR-TKI-A9(B8) combination exhibited enhanced anticancer effects in NCI-H1975 cells harboring L858R and T790M mutations, which were due to simultaneous suppression of extracellular signal–regulated kinases phosphorylation. Our results suggested that targeting ADAM17 could potentiate the anticancer effects of EGFR-TKI against NSCLC and overcome drug resistance due to EGFR mutations.

Translational Oncology (2019) **12**, 1516–1524

Introduction

ADAM17, one of the proteases in the a disintegrin and metalloproteinases (ADAM) family, has received considerable attention recently [1]. The function of ADAM17, or tumor necrosis factor-α (TNF-α)–converting enzyme, has widely been reported as a membrane-bound shedding proteinase, which cleaves proligand proteins or receptors on the cell surface, such as TNF-α, transforming growth factor-α (TGF-α), epidermal growth factor (EGF), interleukin-6 receptor, tumor necrosis factor receptor, and many others, as well as adhesion proteins such as L-selectin or intercellular adhesion molecule-1 [2]. In non–small cell lung cancer (NSCLC), the gene expression of ADAM17 is significantly higher in cancer tissues compared to that of noncancerous tissues. Moreover, higher levels of ADAM17 expression are often associated with poor prognosis in a 5-year overall survival rate [3]. Enhanced expression of ADAM17 by higher levels of estradiol in A549, an NSCLC cell line, was reported to impair the cytotoxicity caused by natural killer cells, indicating that the overexpression of ADAM17 would lead to immune escape in NSCLC [4]. Furthermore, ADAM17 activation has been reported to contribute to the migration and invasion of NSCLC [5]. Silencing of ADAM17 attenuated cell invasion and induced epithelial-to-mesenchymal transition (EMT) [6], while targeting ADAM17 with restoration of miR-152 significantly decreased proliferation, colony formation, migration, and invasion of NSCLC cells [7], suggesting that higher levels of ADAM17 expression are correlated with the initiation and development of NSCLC.

Recently, A9(B8), an anti-ADAM17 IgG$_2$ antibody, has been reported to suppress ADAM17-dependent growth factor shedding [8]. In particular, A9(B8) is a "mouse and human cross-reactive" specific anti-ADAM17 antibody exhibiting murine ADAM17

immunoreactivity, which facilitates the evaluation of the antibody in human xenograft models [8]. Previous enzymatic studies had shown that A9(B8) produced potent and specific anti-ADAM17 activity, with a K_D value of 0.33 nM and an IC_{50} of 0.22 and 0.25 nM against human and mouse ADAM17, respectively [8,9]. These results drove us to pursue the antitumor effect of A9(B8) on a pancreatic ductal adenocarinoma model both *in vitro* and *in vivo*, in which we found that suppression of ADAM17 with A9(B8) significantly attenuated the shedding of some inflammatory and growth factors, such as TNF-α, TGF-α, and amphiregulin (AREG), both *in vitro* and *in vivo* [10]. It is noteworthy that approximately 40% of mice harboring deficiencies of three inflammatory cytokines, namely, granulocyte-macrophage colony-sti-mulating factor, interleukin-3, and interferon-γ, were reported to have chronic pulmonary inflammation and pulmonary alveolar proteinosis, and would develop invasive pulmonary adenocarcinomas when they were crossed onto the lung cancer-susceptible BALB/c background mice [11], highlighting the important roles of multiple inflammatory pathways in lung cancer progression.

It has been reported that over 80% of all lung cancer cases were NSCLC [12]. Approximately 30%-40% of NSCLC patients harbor an epidermal growth factor receptor (EGFR) mutation [12], which promotes the constant phosphorylation of EGF receptors; activates downstream signaling pathways such as RAS-RAF-MEK-ERK, PI3K-AKT-mTOR, and JAK-STAT; and confers cancer cell proliferation and survival [13]. Therefore, targeting EGFR by tyrosine kinase inhibitors (TKIs) is a promising treatment option for EGFR mutant NSCLC patients [14], as demonstrated by the successful applications of the first-generation EGFR-TKIs, gefitinib or erlotinib, which were designed to bind reversibly to the EGFR kinase ATP binding site harboring exon 19 deletions and exon 21 L858R mutations [15]. However, following a period of treatment with EGFR-TKI, acquired resistances often occur in lung cancer cells [16], which are predominantly due to secondary mutations in EGFR, bypassing the alternative pathway activation or histologic transforma-tion [17]. Second and third generations of irreversible EGFR-TKIs, as exemplified respectively by afatinib and osimertinib, have been developed more recently to tackle some of the known secondary mutations, such as exon 20 T790M [18,19]. Although acquired resistance against the third-generation EGFR-TKI has yet to be reported, it is likely to emerge with time in NSCLC patients. Drug combinations appear to be a promising strategy to overcome the acquired resistance in EGFR-TKI therapies [20].

Given the important roles of inflammation in lung cancer, suppression of ADAM17 shedding could attenuate the inflammatory and growth factors that may otherwise facilitate cancer growth. Herein, we hypothesized that the combined use of A9(B8) antibody and a first-generation EGFR-TKI may offer enhanced anticancer effects against NSCLC cells with secondary mutation, such as T790M. Three NSCLC cell lines, namely, NCI-H1975, NCI-H1650, and A549, with different EGFR mutations were used as *in vitro* models to evaluate the drug combination.

Materials and Methods

A9(B8) Antibody Preparation

Human anti-AD0AM17 antibody A9(B8) was produced as previously described [8]. Briefly, expression of A9(B8) IgG was performed by transfection in HEK293 cells, while the antibody in conditioned media was then purified by two Protein-A/G columns

(GE Healthcare) and AKTA FPLC affinity chromatography (GE Healthcare), followed by dialysis in HEPES-buffered saline (pH 7.4) after filter sterilization. Human plasma IgG (R&D System, Car#: 1-001-A) was used as control for assays.

Cell Lines and Reagents

Human NSCLC cell lines NCI-H1975 (Cat#: CRL-5908), NCI-H1650 (Cat#: CRL-5883), and A549 (Cat#: CRM-CCL-185) were purchased from the American Type Culture Collection. Authenticity of NCI-H1975 was certified by STR sequencing analysis (Biowing Biotechnology Co. Ltd., Shanghai). A549 cells were cultured in DMEM (Gibco, ThermoFisher Scientific, Cat#: 12100061), while other cells were maintained in RPMI 1640 (Gibco, ThermoFisher Scientific, Cat#: 31800089). All culture media were supplemented with 10% fetal bovine serum (Gibco, ThermoFisher Scientific, Cat#: 10270098). Cells were maintained in a humidified atmosphere with 5% CO_2 at 37°C in incubators.

Erlotinib was purchased from Cayman Chemical (Cat#: 10483). Gefitinib was purchased from SelleckChem (Cat#: S1025). Anti--ADAM17 primary antibody was ordered from Abcam (Cat#: ab39162). The primary antibodies against α-tubulin (Cat#: A11126) or GAPDH (Cat#: MA5-15738) were purchased from Invitrogen, while all other antibodies, including phospho-EGFR (Cat#: 2236S), EGFR (Cat#: 4267S), phospho-ERK (Cat#: 9101S), ERK (Cat#: 9102S), and β-actin (Cat#: 4967), were purchased from Cell Signaling Technology. Control human plasma IgG was purchased from R&D Systems (Cat#: 1-001-A). All other chemicals were purchased from Sigma or Sigma-Aldrich.

Cell Viability Assay

Cell viability of each individual treated or nontreated sample was determined by the 3-(4, 5-dimethylthiazol-2-yl)-2,5-diphenyl tetra-zolium bromide (MTT, Sigma, Cat#: M2128) assay. Briefly, NCI-H1975 (3000 cells/well), NCI-H1650 (7000 cells/well), or A549 (3000 cells/well) cell lines were seeded in 96-well plates and incubated for 24 hours to allow for cell attachment. Cells were then exposed to either erlotinib/gefitinib or A9(B8), either individually or in combination, for 72 hours. After treatment, culture media were refreshed with 100 μl of whole media containing 0.5 mg/ml MTT. After 4 hours of incubation, the solvent was discarded, and 100 μl DMSO was added to allow the dissolution of formazan crystals. Then, plates were measured at 570 nm with a SpectraMax M5 Microplate Reader (Molecular Devices) for O.D. value determination.

Western Blotting Assay

Alternations in specific cell signaling pathways, caused by different treatments, were investigated by immunoblotting. Briefly, NCI-H1975 cells (300,000 cells/well) were seeded in six-well plates and incubated for 24 hours to allow for cell attachment. Then, the cells were initially treated with or without phorbol 12-myristate 13-acetate (PMA, Sigma, Cat#: 79346) at a concentration of 25 nM for 20 minutes, followed by exposing to either erlotinib/gefitinib or A9(B8), either individually or in combination, at varying concentrations for 6 or 12 hours, respectively. The treated cells were then harvested and lysed in 1× lysate buffer (Cell Signaling Technology, Cat#: 9803S) containing a protease/phosphatase inhibitor cocktail (Cell Signaling Technology, Cat#: 5872S) for 15 minutes, followed by centrifugation at 13,000 ×g at 4°C for 20 minutes. Protein concentration of each sample was assessed using the
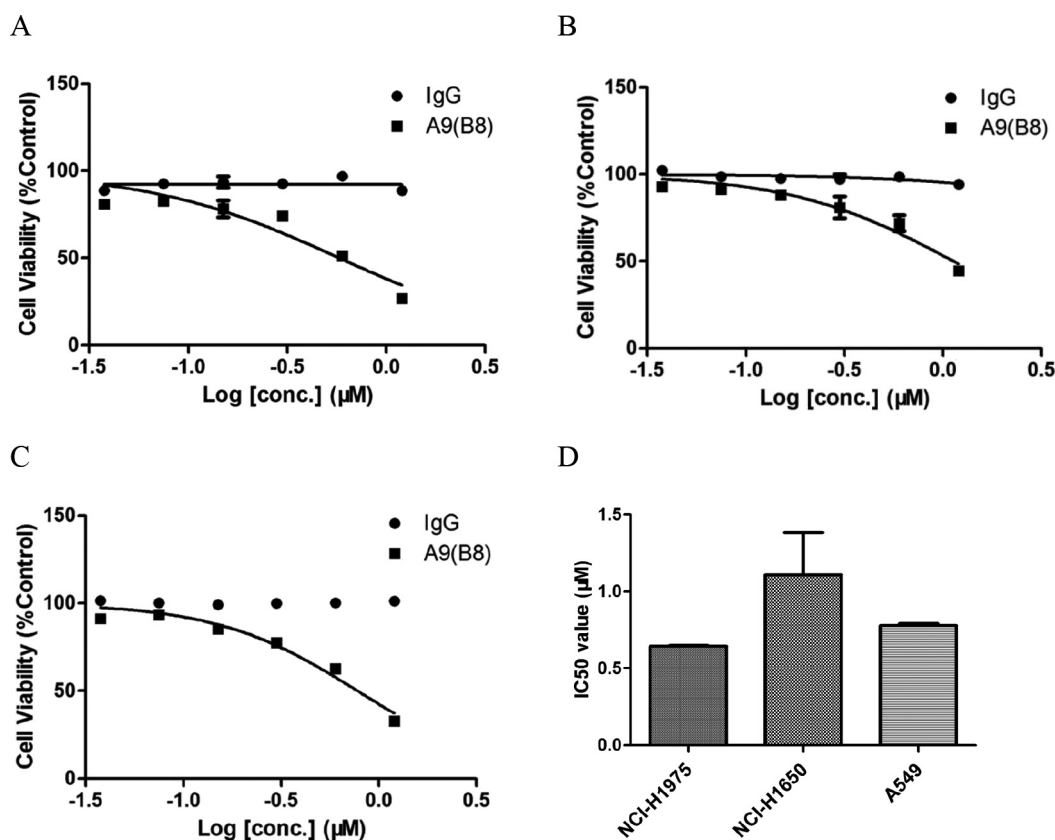
Figure 1. A9(B8) attenuated cell viability in NSCLC cells. MTT assays were performed to determine loss of cell viability by A9(B8) in NCI-H1975 (A), NCI-H1650 (B), and A549 (C) cells. IC_{50} values of A9(B8) in the three cell lines (D) were calculated by using Prism Graph Pad 5.1. MTT assays were performed with four duplicated wells for each sample. IC_{50} data were presented as mean ± SD. Human plasma IgG was utilized as the control.

Pierce BCA Protein Assay Kit (ThermoFisher Scientific, Cat#: 23325) and adjusted to a mean level. Then, the treated samples were denatured at 100°C after mixing with SDS loading buffer and stored at −20°C for further use. For immunoblotting assays, samples were run on 10% SDS-polyacrylamide gels for separation and then transferred to nitrocellulose membranes (Pall) using the Mini-Protean Tetra Electrophoresis and Trans-Blot System (Bio-Rad). Membranes were then blocked in 5% fat-free milk for 2 hours followed by overnight incubation in the indicated primary antibodies at 4°C and sequent incubation with the appropriate anti-rabbit or anti-mouse HRP-linked IgG secondary antibody for 1 hour at room temperature. Visualized signals from the membranes were developed using the Chemidocs MP Imaging System (Bio-Rad) after 2-minute incubation in Clarity Western ECL Substrate (Bio-Rad). Semiquantitative analysis of individual bands was performed using ImageJ.

Statistical Analysis

All data are presented as mean ± SD. Differences in IC_{50} values comparison between different sample groups were performed through Excel using Student's *t* test. A *P* value of less than .05 was considered significant.

Results

Anticancer Activities of A9(B8) in Human NSCLC Cell Lines

We first studied the anticancer activity of A9(B8) antibody in human NSCLC. Three NSCLC cell lines, namely, NCI-H1975, NCI-H1650, and A549, were selected as *in vitro* models in which MTT assays were performed to determine the IC_{50} of A9(B8). Normal human IgG was

used as the control. According to the COSMIC Cell Lines Project (https://cancer.sanger.ac.uk/cell_lines/cbrowse/all, accessed 15 Nov 2018), A549 cells do not show any EGFR mutation, while NCI-H1975 cells harbor L858R/T790M mutations and NCI-H1650 cells harbor exon 19 mutation (E746_A750delELREA). As shown in Figure 1, the A9(B8) antibody had a modest effect on cell viability in all of the cells (Figure 1, A, B, and C), with IC_{50} mean values of 0.65, 1.11, and 0.78 µM in NCI-H1975, NCI-H1650, and A549 cells, respectively (Figure 1D). In contrast, an IgG control did not affect the viability in those cells, indicating that A9(B8) elicited significant anticancer effects in NSCLC therapy *in vitro*.

Combined Use of A9(B8) and EGFR-TKI for Evaluating Anti-Cancer Effects

Next, we direct our attention to the combined use of A9(B8) and EGFR-TKI with the aim of evaluating the anticancer effects in NSCLC models. Specifically, MTT assays were performed in NCI-H1975, NCI-H650, and A549 cell lines, where the cells were treated with either erlotinib or gefitinib, two first-generation EGFR-TKIs, in the presence or absence of A9(B8) antibody or IgG control protein. Figure 2, A and B showed a dramatic decrease in IC_{50} value of either erlotinib or gefitinib in NCI-H1975 cells in the presence of A9(B8) antibody at a concentration of 0.3 µM, with significant differences (*P* < .05) compared to either EGFR-TKI treated alone or in the presence of IgG control. In marked contrast, the combination revealed different pictures in NCI-H1650 or A549 cells. For instance, IgG control did not exhibit any effects on the anticancer activity of erlotinib
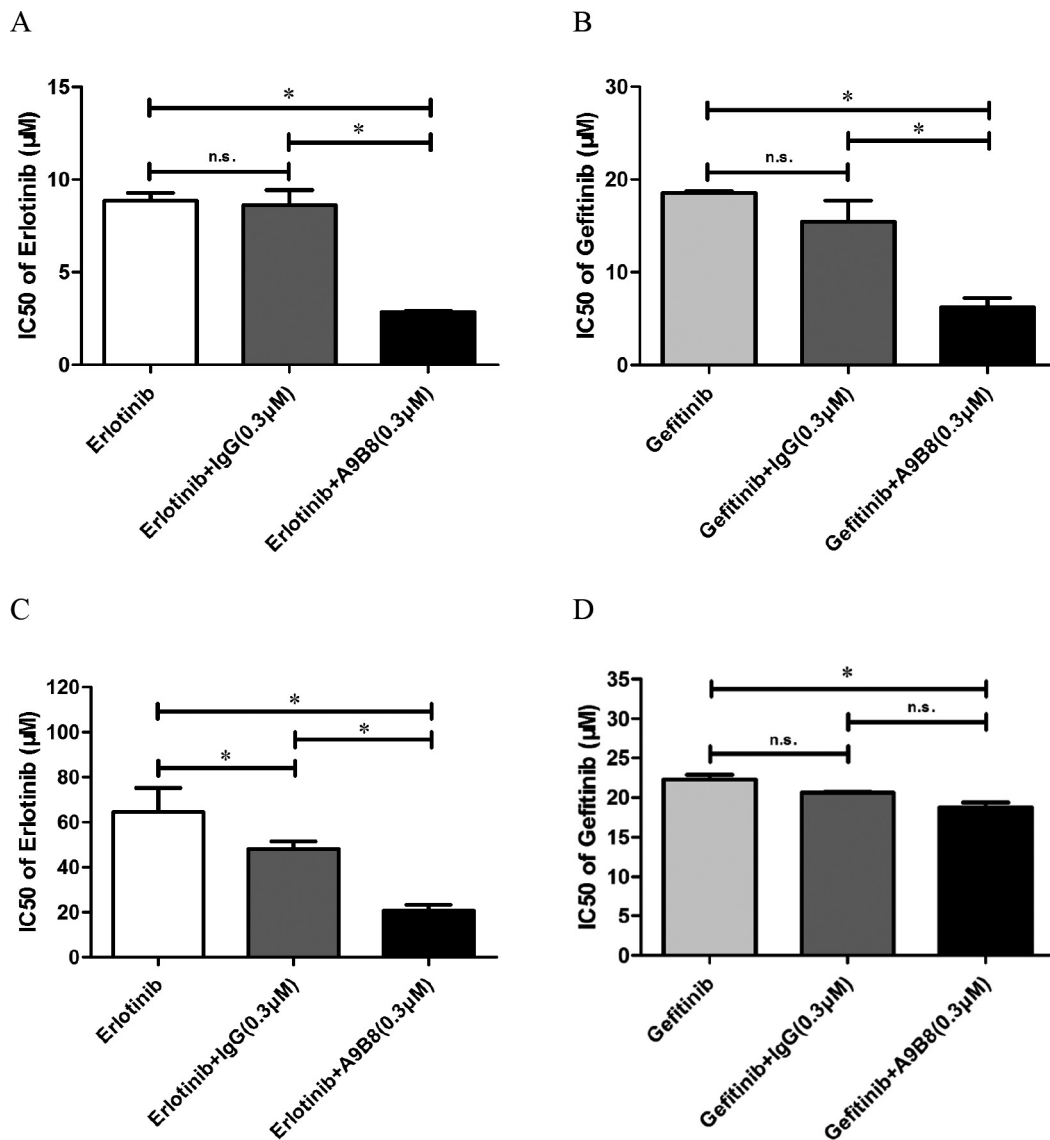
Figure 2. Introduction of A9(B8) enhanced the anticancer effect produced by EGFR-TKI application in NSCLC cells. MTT viability assays were performed to determine the change in IC_{50} values of erlotinib/gefitinib in NCI-H1975 (A and B), NCI-H1650 (C and D), and A549 (E and F) cells after A9(B8) was introduced. Immunoblotting assays were performed to compare the differences in endogenous protein expression or phosphorylation among the three cell lines (G) with the performance of relative ratio within p-EGFR/EGFR (H) and ADAM17/tubulin (I) using semiquantitative analysis. MTT assays were performed with four duplicated wells for each sample. IC_{50} data were calculated by using Prism Graph Pad 5.1 and presented as mean ± SD. Human plasma IgG was utilized as the control. Semiquantitative analysis of individual bands was performed using ImageJ. $*P < .05$ between compared groups. n.s. represents no significance between groups.

(Figure 2, C and E), and the presence of A9(B8) did not reduce the IC_{50} values of gefitinib in MTT assays (Figure 2, D and F). To shed light on this discrepancy, we utilized immunoblotting assays to determine the expression of ADAM17 and EGFR phosphorylation. As shown in Figure 2, G-I, NCI-H1975 exhibited the highest expression level of ADAM17 and the most activated EGFR compared to the two other NSCLC cell lines. In the subsequent discussion, we focused our pharmacological investigations using NCI-H1975 cells.

Combination of A9(B8) and EGFR-TKI Inhibiting ERK Phosphorylation

We then determined the effects of A9(B8) on phosphorylation of EGFR and its downstream ERK in both dose- and time-dependent manner. Therein, A9(B8) alone did not produce any impact on either EGFR or ERK phosphorylation (Figure 3A). Further immunoblotting assays were performed to detect whether there would be an enhancement in erlotinib-treated NCI-H1975 signaling suppression in the presence of A9(B8). As shown in Figure 3, B and C, erlotinib alone can suppress EGFR and ERK phosphorylations (Figure 3B), while the combined use of A9(B8) and erlotinib demonstrated a further attenuation of ERK phosphorylation compared to the single use of erlotinib (Figure 3C). However, further attenuation of EGFR phosphorylation was not observed in the combination treatment. It is plausible that the attenuation of ERK phosphorylation would be the key factor for the enhancement of the anticancer effects by the combination of A9(B8) and of erlotinib.
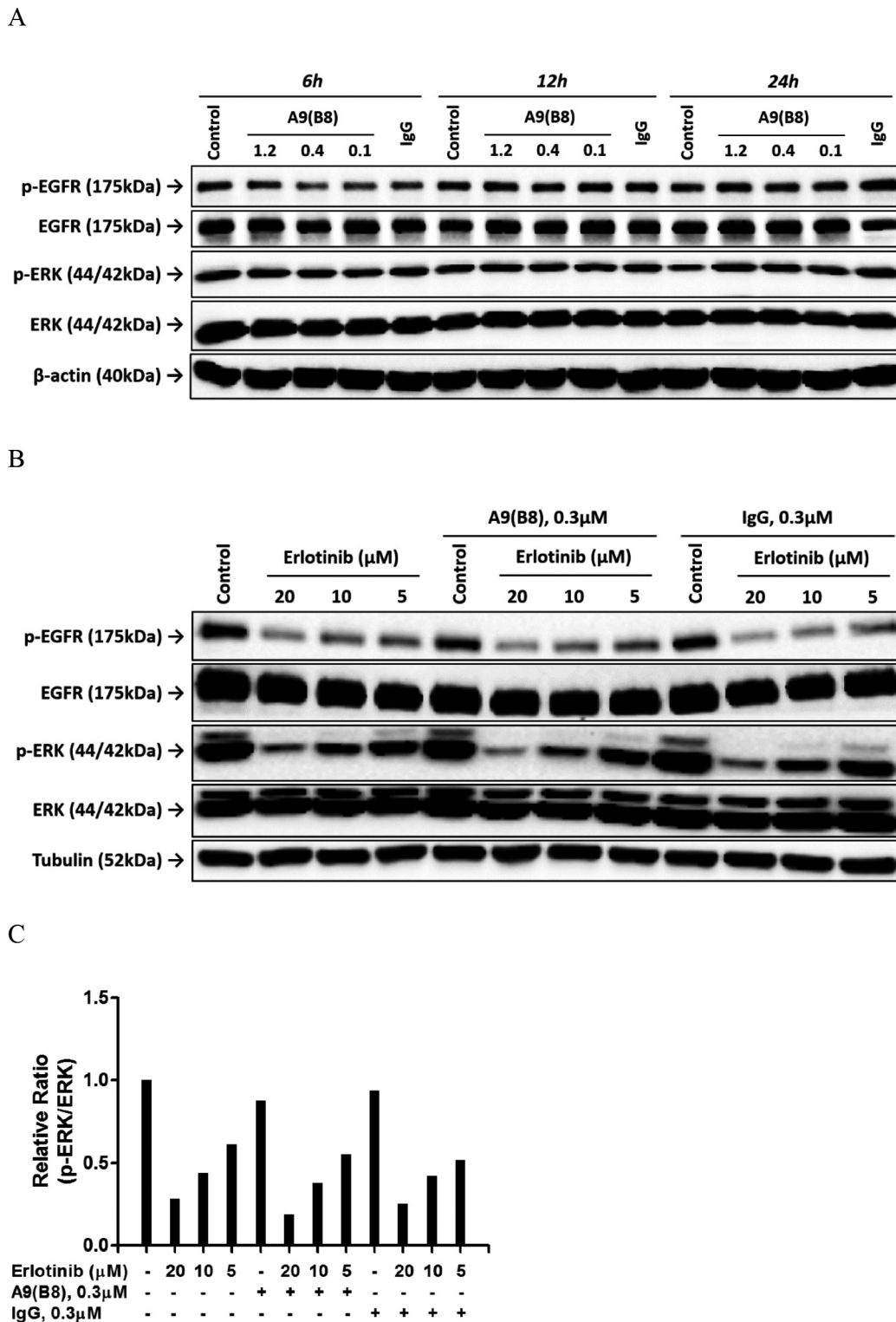
Figure 3. Effect of A9(B8) and erlotinib on EGFR and ERK phosphorylations. Immunoblotting assays were performed to determine the effects of compound and antibody on EGFR or ERK phosphorylation in NCI-H1975 cells. (A) NCI-H1975 cells were treated with A9(B8) in a dose-dependent manner for 6, 12, and 24 hours. Cells without treatment (control) or treated with IgG at a concentration of 1.2 μM (IgG) were utilized as the individual control for the defined time. (B) NCI-H1975 cells were treated with erlotinib in a dose-dependent manner in the presence or absence of 0.3 μM A9(B8) for 12 hours. (C) Relative ratio between p-ERK and ERK in B. IgG at a concentration of 0.3 μM was utilized as the control.

PMA Stimulation Further Attenuating ERK Phosphorylation in the Drug Combination

PMA is a potent activator of protein kinase C, which could induce the ADAM17 activity leading to cancer progression [21]. Previously, we utilized PMA to induce the release of ADAM17 shed substrates, which enabled us to observe the attenuation of these ligands in culture media when anti-ADAM17 antibodies were applied [10]. Moreover, application of PMA was also reported to be associated with induction
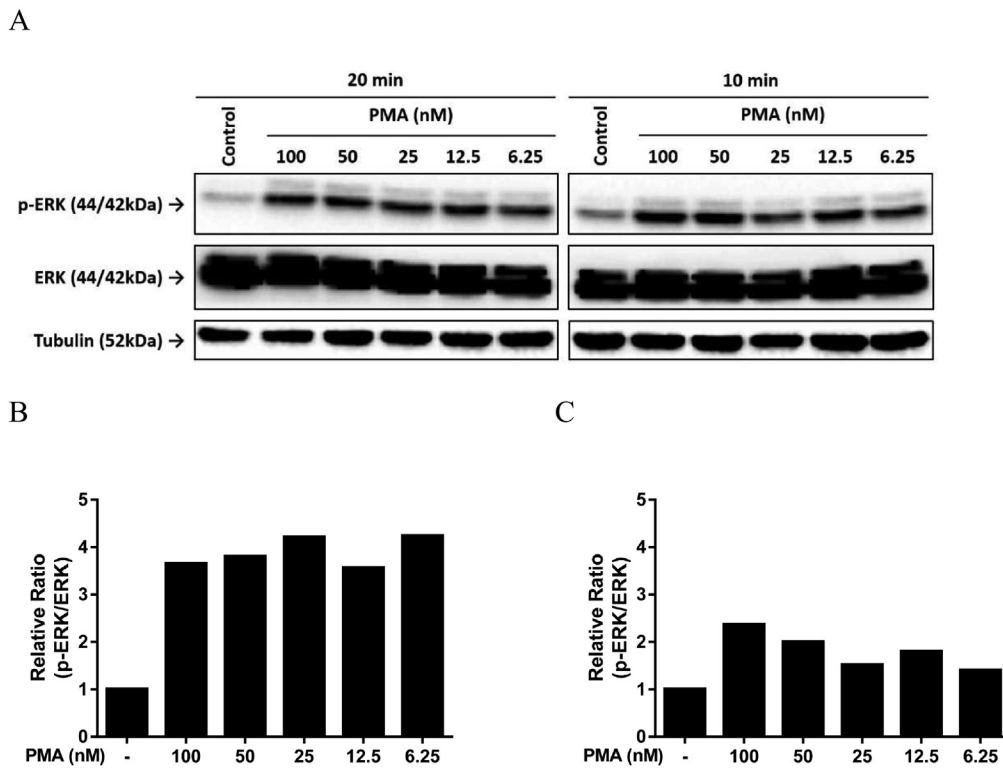
Figure 4. PMA stimulated ERK phosphorylation. Immunoblotting assays (A) and the following semiquantitative analysis (B and C) were performed to determine the effects of PMA on ERK phosphorylation in NCI-H1975 cells. NCI-H1975 cells were treated by PMA in a dose-dependent manner for the defined time of 20 minutes (B) or 10 minutes (C).

of ERK phosphorylation [22]. It would be of great interest to evaluate whether the combined use of A9(B8) and EGFR-TKI in NCI-H1975 cells with prior PMA stimulation could attenuate ERK phosphorylation. In the absence of drug treatment, we first examined the dose-response and time-course of PMA-mediated ERK activation (Figure 4A). As shown in Figure 4, B and C, 20-minute stimulation exhibited considerably higher p-ERK/ERK ratios compared to those of 10-minute stimulation. Based on this observation, we utilized PMA at 25 nM with 20-minute stimulation prior to EGFR-TKI and A9(B8) application. As shown in Figure 5, the presence of A9(B8) in either erlotinib- or gefitinib-treated NCI-H1975 cells produced further attenuation of ERK phosphorylation compared to either EGFR-TKI alone or IgG control, even under the stimulation of PMA. Without PMA stimulation, the combined use of A9(B8) and erlotinib (or gefitinib) induced much stronger attenuation of ERK phosphorylation.

Discussion

We first studied the anticancer activity of A9(B8) antibody in NSCLC cell lines, namely, NCI-H1975, NCI-H1650, and A549. The A9(B8) antibody exhibited a modest antiproliferative effect in all of the cell lines (Figure 1). In the combined use of A9(B8) antibody and EGFR-TKI, we have observed that A9(B8) at a concentration of 0.3 μM potentiated the anticancer effects of EGFR-TKI by reducing its IC$_{50}$ values. However, the extent of potentiation was found to be cell line dependent, with the effect being most significant in NCI-H1975 cells (Figure 2, A and B). To rationalize this observation, we examined the expression of ADAM17 and EGFR phosphorylation among these cell lines, and it was found that NCI-H1975 exhibited

the highest expression level of ADAM17 and the most activated EGFR compared to the two other NSCLC cell lines (Figure 2, G-I). Besides EGFR and ADAM17 activation, NCI-H1650 harbors mutation of PTEN null, which enables consecutive PI3K/mTOR pathway activation [23]. A549, on the other hand, harbors Kras mutation so that EGFR-TKI cannot suppress ERK phosphorylation *via* targeting EGFR [24,25]. We hypothesized that the highly activated EGFR and overexpressed ADAM17 are the necessary conditions for A9(B8) to potentiate the anticancer effects of EGFR-TKI in NSCLC cells.

In NCI-H1975 cells, we have observed that the use of erlotinib alone inhibited both EGFR and ERK phosphorylations (no effect observed when A9(B) was used alone). In the combined use of erlotinib and A9(B8), further attenuation of ERK phosphorylation was observed compared to the single use of erlotinib (Figure 3, B and C). Moreover, we have applied PMA stimulation in NCI-H1975 cells to induce the release of ADAM17 shed substrates such as HB-EGF and TGF-α (Supplementary Figure 1). We have shown that A9(B8) and erlotinib (or gefitinib) combination further suppressed ERK phosphorylation compared to either EGFR-TKI alone or IgG control (Figure 5), even under prior PMA stimulation. This justifies the effectiveness and the specificity of the combined use of A9(B8) and EGFR-TKI to suppress ERK phosphorylation. Our results clearly suggest that A9(B) potentiates the anticancer effect of EGFR-TKI in NCI-H1975 cells through the enhanced suppression of ERK phosphorylation.

EGFR mutations exhibited ligand-independent EGFR signaling and tumor growth in NSCLC and glioblastoma patients [26,27]. As shown in previous studies, inhibitions of the shedding of TNF-α by
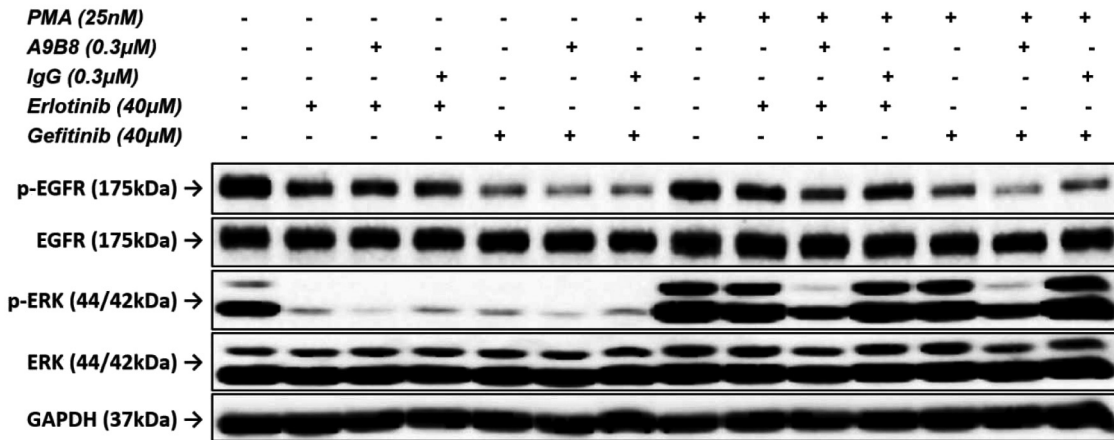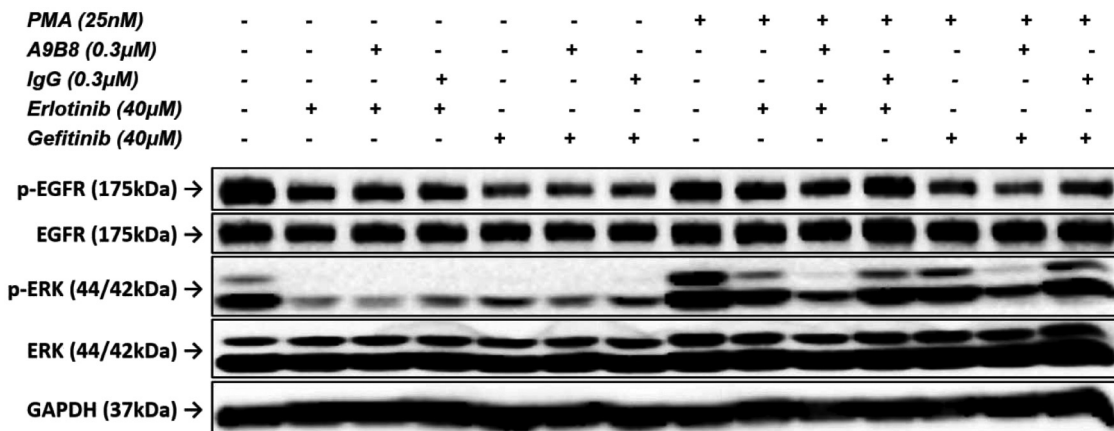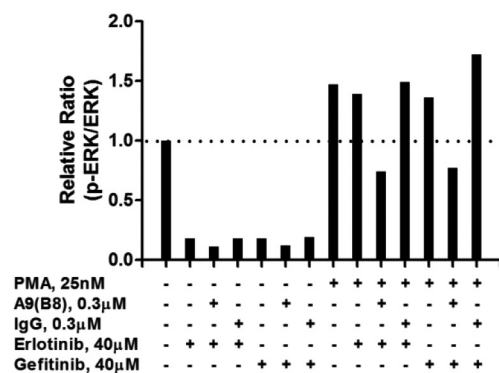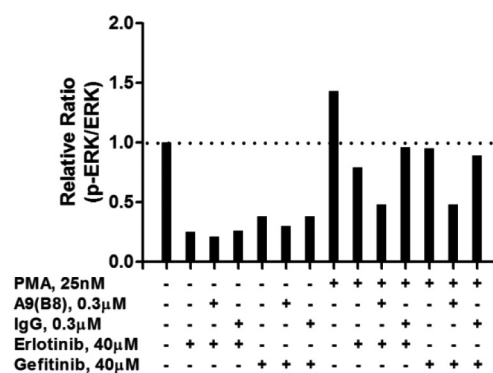
Figure 5. Introduction of A9(B8) further attenuated ERK phosphorylation suppressed by EGFR-TKI in NCI-H1975 cells. Immunoblotting assays were performed to determine the effects of compound/antibody, either individually or in combination, on EGFR or ERK phosphorylation in NCI-H1975 cells. NCI-H1975 cells were treated for 6 (A) or 12 hours (B) with whole media containing compound/antibody in the presence or absence of PMA stimulation. (C and D) Relative ratio between p-ERK and ERK in A and B. Human plasma IgG was utilized as the control.

anti-ADAM17 antibodies have been observed in various cancer models, including ovarian [28], head and neck [29], and pancreas [10]. It is plausible that the effects of ADAM17 inhibition *via* A9(B8) are due to the reduction of the shedding of inflammatory factor, for

example, TNF-α (Supplementary Figure 2), leading to the suppression of ERK phosphorylation as observed in our drug combination treatment against NCI-H1975. Activation of the MAPK/ERK pathways by TNF-α in mouse macrophages has already been reported
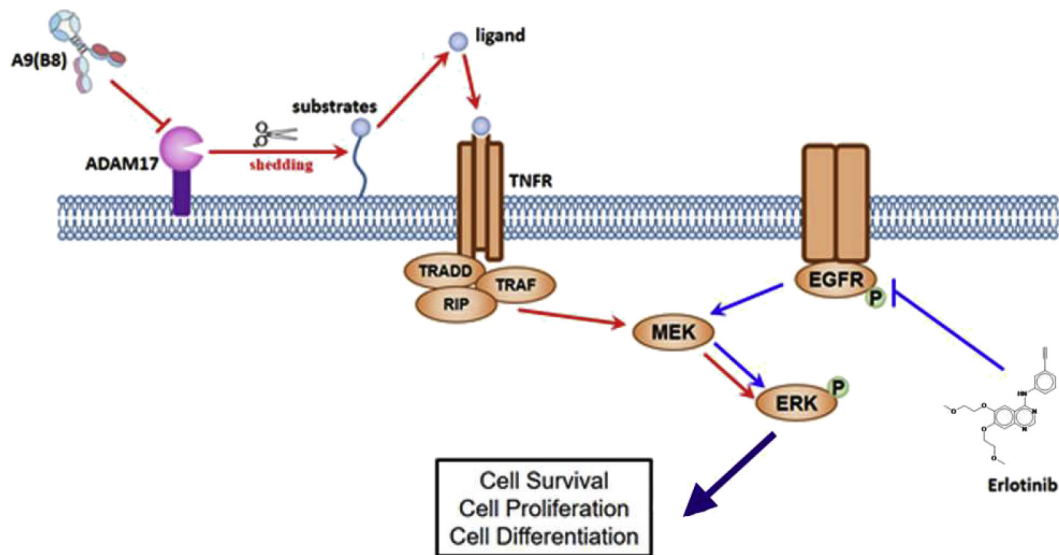
Figure 6. Proposed schematic model in the current study. EGFR-TKI produces anticancer effects through targeting EGFR phosphorylation and suppressing the downstream ERK activation. Introduction of A9(B8) inhibits ADAM17 activity, decreases ADAM17-mediated TNF-α proligands shedding, and reduces the downstream ligands-dependent TNF receptor signaling activation, all of which contribute to the further attenuation of ERK phosphorylation, resulting in the enhanced anticancer effects.

[30]. Of note, NCI-H1975 cell line harbors the T790M mutation, which is known to compromise the antiproliferative effects of erlotinib. Nevertheless, enhanced anticancer effects were observed in the presence of A9(B8), suggesting that the shedding of inflammatory factors potentiates the effectiveness of a first-generation EGFR-TKI in an EGFR-mutant NSCLC cell line harboring T790M. In corroboration with our observation, a recent study has reported that simultaneous inhibition of TNF-α and EGFR is effective in NSCLC with acquired resistance to EGFR inhibition [31]. Clearly, the role of attenuated shedding of inflammatory factors *via* A9(B8) in combination of different generations of EGFR-TKIs against NSCLC deserves further investigation, which will be a subject of our forthcoming publication.

In our previous study, we have evaluated the *in vivo* behavior of A9(B8) in mice [10]. Pharmacokinetic studies of A9(B8) were carried out over a dosing period of 42 days without any obvious side effects. The initial and terminal half-lifes of A9(B8) in mouse were found to be 13.0 hours and 10.5 days, respectively [10]. Moreover, we applied A9(B8) in a transgenic pancreatic cancer mouse model and found that it could delay tumorigenesis and attenuate the progression of preinvasive pancreatic lesions by decreasing some inflammatory factors [10]. Based on this observation, it is expected that A9(B8) may not work well in the NCI-H1975 xenograft model that we developed previously for evaluating the anticancer effects in drug combination study [32]. We are currently developing lung cancer mouse models of inflammatory origin [11] to investigate the antitumor efficacy of the combined use of A9(B8) and different generations of EGFR-TKIs. The results will be reported in due course.

In summary, we characterized the anticancer activity of A9(B8), an anti-ADAM17 mutant IgG antibody, in NSCLC *in vitro* models. Moreover, we have shown that the presence of the antibody increased the sensitivity of EGFR-mutant NSCLC cells to EGFR-TKI treatments, which was due to the reduction of ADAM17-mediated shedding of inflammatory substrates, leading to the decrease in the activation of ERK phosphorylation (Figure 6). Our data provide compelling evidence to support further *in vivo* anticancer efficacy evaluation of the A9(B8) and EGFR-TKI combination in preclinical lung cancer models.

Conflict of Interest
None of the authors declare any conflict of interest.

Appendix A. Supplementary data
Supplementary data to this article can be found online at https://doi.org/10.1016/j.tranon.2019.08.003.

References

[1] Miller MA, Sullivan RJ and Lauffenburger DA (2017). Molecular pathways: receptor ectodomain shedding in treatment, resistance, and monitoring of cancer. *Clinical cancer research : an official journal of the American Association for Cancer Research* **23**, 623−629.

[2] Scheller J, Chalaris A, Garbers C and Rose-John S (2011). ADAM: a molecular switch to control inflammation and tissue regeneration. *Trends Immunol* **32**, 380−387.

[3] Ni SS, Zhang J, Zhao WL, Dong XC and Wang JL (2013). ADAM17 is overexpressed in non-small cell lung cancer and its expression correlates with poor patient survival. *Tumour Biol* **34**, 1813−1818.

[4] Ren J, Nie Y, Lv M, Shen S, Tang R, Xu Y, Hou Y, Zhao S and Wang T (2015). Estrogen upregulates MICA/B expression in human non-small cell lung cancer through the regulation of ADAM17. *Cell Mol Immunol* **12**, 768−776.

[5] Lv X, Li Y, Qian M, Ma C, Jing H, Wen Z and Qian D (2014). ADAM17 silencing suppresses the migration and invasion of non-small cell lung cancer. *Mol Med Rep* **9**, 1935−1940.

[6] Cai M, Wang Z, Zhang J, Zhou H, Jin L, Bai R and Weng Y (2015). Adam17, a target of Mir-326, promotes Emt-induced cells invasion in lung adenocarcinoma. *Cell Physiol Biochem* **36**, 1175−1185.

[7] Su Y, Wang Y, Zhou H, Lei L and Xu L (2014). MicroRNA-152 targets ADAM17 to suppress NSCLC progression. *FEBS Lett* **588**, 1983−1988.

[8] Kwok HF, Botkjaer KA, Tape CJ, Huang Y, McCafferty J and Murphy G (2014). Development of a 'mouse and human cross-reactive' affinity-matured

exosite inhibitory human antibody specific to TACE (ADAM17) for cancer immunotherapy. *Protein Eng Des Sel* **27**, 179−190.

[9] Takayanagi T, Forrester SJ, Kawai T, Obama T, Tsuji T, Elliott KJ, Nuti E, Rossello A, Kwok HF and Scalia R, et al (2016). Vascular ADAM17 as a novel therapeutic target in mediating cardiovascular hypertrophy and perivascular fibrosis induced by angiotensin II. *Hypertension* **68**, 949−955.

[10] Ye J, Yuen SM, Murphy G, Xie R and Kwok HF (2017). Anti-tumor effects of a 'human & mouse cross-reactive' anti-ADAM17 antibody in a pancreatic cancer model in vivo. *Eur J Pharm Sci* **110**, 62−69.

[11] Dougan M, Li D, Neuberg D, Mihm M, Googe P, Wong KK and Dranoff G (2011). A dual role for the immune response in a mouse model of inflammation-associated lung cancer. *J Clin Invest* **121**, 2436−2446.

[12] Ke EE, Zhou Q and Wu YL (2015). Emerging paradigms in targeted treatments for Asian patients with NSCLC. *Expert Opin Pharmacother* **16**, 1167−1176.

[13] Zhang Z, Stiegler AL, Boggon TJ, Kobayashi S and Halmos B (2010). EGFR-mutated lung cancer: a paradigm of molecular oncology. *Oncotarget* **1**, 497−514.

[14] Hanahan D and Weinberg RA (2011). Hallmarks of cancer: the next generation. *Cell* **144**, 646−674.

[15] da Cunha Santos G, Shepherd FA and Tsao MS (2011). EGFR mutations and lung cancer. *Annu Rev Pathol* **6**, 49−69.

[16] Pao W and Chmielecki J (2010). Rational, biologically based treatment of EGFR-mutant non-small-cell lung cancer. *Nat Rev Cancer* **10**, 760−774.

[17] Tan CS, Gilligan D and Pacey S (2015). Treatment approaches for EGFR-inhibitor-resistant patients with non-small-cell lung cancer. *Lancet Oncol* **16**, e447−e459.

[18] Wirth SM (2015). Afatinib in non−small cell lung cancer. *J Adv Pract Oncol* **6**, 448−455.

[19] V. Hirsh, Turning EGFR mutation-positive non−small-cell lung cancer into a chronic disease: optimal sequential therapy with EGFR tyrosine kinase inhibitors, Therapeutic advances in medical oncology, 10 (2018) 1758834017753338.

[20] Yang Z and Tam KY (2018). Combination strategies using EGFR-TKi in NSCLC therapy: learning from the gap between pre-clinical results and clinical outcomes. *Int J Biol Sci* **14**, 204−216.

[21] Lorenzen I, Lokau J, Korpys Y, Oldefest M, Flynn CM, Kunzel U, Garbers C, Freeman M, Grotzinger J and Dusterhoft S (2016). Control of ADAM17 activity by regulation of its cellular localisation. *Sci Rep* **6**:35067.

[22] Hwang MN, Ha TH, Park J, Shim J, Lee H, Kim YN, Lee ES and Yoon S (2007). Increased SOCS6 stability with PMA requires its N-terminal region and the Erk pathway via Pkcdelta activation. *Biochem Biophys Res Commun* **354**, 184−189.

[23] Takeda H, Takigawa N, Ohashi K, Minami D, Kataoka I, Ichihara E, Ochi N, Tanimoto M and Kiura K (2013). Vandetanib is effective in EGFR-mutant lung cancer cells with PTEN deficiency. *Exp Cell Res* **319**, 417−423.

[24] Wang Y, Yan P, Liu Z, Yang X, Wang Y, Shen Z, Bai H, Wang J and Wang Z (2016). MEK inhibitor can reverse the resistance to bevacizumab in A549 cells harboring Kirsten rat sarcoma oncogene homolog mutation. *Thorac Cancer* **7**, 279−287.

[25] Yang Z and Tam KY (2016). Anti-cancer synergy of dichloroacetate and EGFR tyrosine kinase inhibitors in NSCLC cell lines. *Eur J Pharmacol* **789**, 458−467.

[26] Guo G, Gong K, Wohlfeld B, Hatanpaa KJ, Zhao D and Habib AA (2015). Ligand-Independent EGFR Signaling. *Cancer Res* **75**, 3436−3441.

[27] Siegelin MD and Borczuk AC (2014). Epidermal growth factor receptor mutations in lung adenocarcinoma. *Lab Invest* **94**, 129−137.

[28] Richards FM, Tape CJ, Jodrell DI and Murphy G (2012). Anti-tumour effects of a specific anti-ADAM17 antibody in an ovarian cancer model in vivo. *PloS one* **7**:e40597.

[29] Huang Y, Benaich N, Tape C, Kwok HF and Murphy G (2014). Targeting the sheddase activity of ADAM17 by an anti-ADAM17 antibody D1(A12) inhibits head and neck squamous cell carcinoma cell proliferation and motility via blockage of bradykinin induced HERs transactivation. *Int J Biol Sci* **10**, 702−714.

[30] Winston BW, Lange-Carter CA, Gardner AM, Johnson GL and Riches DW (1995). Tumor necrosis factor alpha rapidly activates the mitogen-activated protein kinase (MAPK) cascade in a MAPK kinase kinase-dependent, c-Raf-1−independent fashion in mouse macrophages. *Proc Natl Acad Sci U S A* **92**, 1614−1618.

[31] Gong K, Guo G, Gerber DE, Gao B, Peyton M, Huang C, Minna JD, Hatanpaa KJ, Kernstine K and Cai L, et al (2018). TNF-driven adaptive response mediates resistance to EGFR inhibition in lung cancer. *J Clin Invest* **128**, 2500−2518.

[32] Yang Z, Hu X, Zhang S, Zhang W and Tam KY (2017). Pharmacological synergism of 2,2-dichloroacetophenone and EGFR-TKi to overcome TKi-induced resistance in NSCLC cells. *Eur J Pharmacol* **815**, 80−87.